COMPUTER MODELING OF EDDY CURRENT PROBABILITY OF CRACK DETECTION

R.E. Beissner and J.S. Graves, III

Southwest Research Institute
6220 Culebra Road
San Antonio, TX 78228-0510

INTRODUCTION

The objective of this work was to demonstrate the application of eddy current modeling to the determination of the probability of crack detection. The method of calculation, derived from previously reported work on the boundary element method (BEM) [1], used concepts discussed in other works on probability of detection (POD) calculations [2,3]. In contrast to the earlier POD investigations, which were concerned with crack-like flaws in flat plates with a simple circular coil as the probe, the present modeling deals with a realistic part geometry and a split-D probe configuration with ferrite cores and shield. Figures 1 and 2 show the part and probe geometries, respectively; the specifics of the inspection problem are described in the first section of this paper.

While the basic computational approach was essentially the same as that reported last year, a few modifications were introduced to make the complex BEM model tractable and to account for the effects of the ferrite core and shield on the probe field. These enhancements of the model are described in the second section.

The end result of the calculations was the prediction of probe impedance variations for a series of scans over the unflawed part and over regions containing flaws of various sizes and locations. The final two sections describe the set of calculations and the development of POD data from the calculated results.

INSPECTION PROBLEM

Figure 1 shows a model of the front wing-spar lower cap lug for a T37 aircraft. The figure also shows an eddy current probe in the inspection position over the beveled edge at the top of the part. An inspection consists of a series of circular arc scans of the probe over the surface of the beveled edge. Flaws of concern are cracks which tend to occur near the front edge of the beveled surface, as indicated in the figure. The probe is a pair of D-shaped coils wound in opposition around ferrite cores and shielded by a ferrite cylinder, as shown in Figure 2.

Review of Progress in Quantitative Nondestructive Evaluation, Vol. 9
Edited by D.O. Thompson and D.E. Chimenti
Plenum Press, New York, 1990

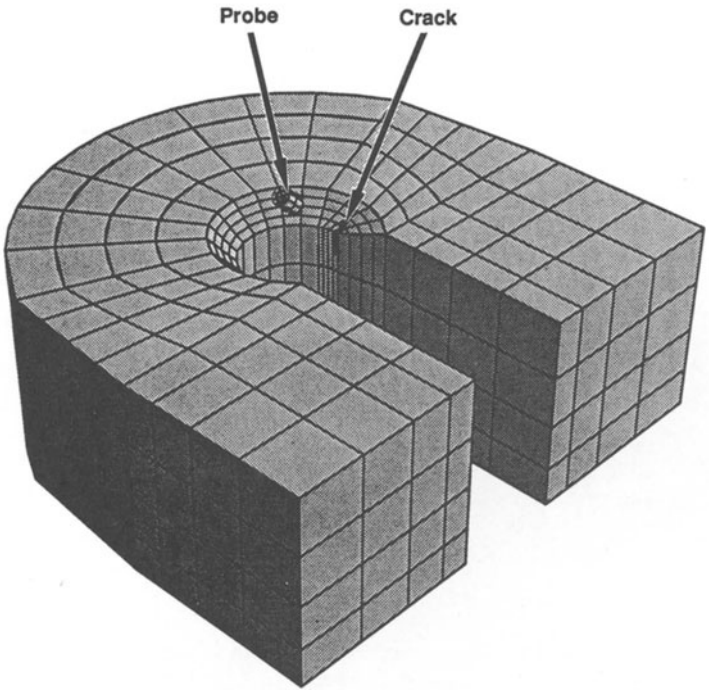

Fig. 1. Eddy current inspection of the T37 front wing-spar lower cap lug. The probe is scanned in a circular arc over the beveled edge of the part. Cracks tend to occur in the region indicated.

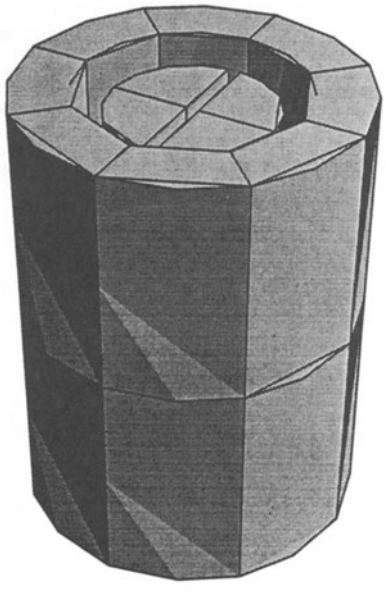

Fig. 2. Model of a split-D ferrite core probe with a ferrite shield.

With a split-D differential probe of the type used here, an ideal crack signal is a figure-8 impedance locus, generated as the pair of coils pass over the flaw. Crack detection relies on the generation of such a pattern and the ability of the inspector to recognize it. The particular difficulty posed by the inspection problem illustrated in Figure 1 is that cracks occur near the edge of the beveled surface. This results in probe impedance changes due to the proximity of the edge, which tend to mask flaw signals and distort the figure-8 pattern associated with crack detection. The probability of crack detection is, therefore, intimately related to the geometry of the part, necessitating a three-dimensional model in the computer simulation of the inspection. The POD also depends on the signal-recognition capability of the inspector, and this means that a realistic simulation must also involve the generation of impedance loci and their interpretation by qualified inspectors.

The task of modeling the inspection was accomplished in two steps: first, computation of the impedance loci for probe scans over flawed and unflawed parts and, second, examination and interpretation of these computed figures for evidence of flaw signals.

BEM MODEL

The BEM approach to modeling eddy current probe response was described in an earlier report [1]. The impedance formula is the reciprocity integral [4], written in terms of the magnetic scalar potential on the surface of the part and the free-space field of the probe. A three-dimensional BEM code provides the surface potential, and the free-space probe potential is determined by a separate calculation. In the configuration of interest here, the presence of ferrites complicates the free-space field; and a new approach, described below, was required.

As is evident on comparison of Figure 1 with the BEM models considered in our last report, the mesh required to model even the unflawed part is much more complex in the present case. In fact, more than 1500 nodal points occur in the mesh shown in Figure 1. To introduce a small, crack-like flaw by straightforward modification of the mesh would require a very large increase in the number of nodes, thus making the computation impractical. To avoid this situation, the problem was treated in two steps, taking advantage of the fact that the field perturbation caused by a small flaw is highly localized, and the field outside a region of influence around the flaw can be assumed to be unperturbed.

The boundary integral equation that embodies this approximation is the following:

$$\left[1 - \int_S \frac{dG(\vec{x},\vec{x}')}{dn'} dS'\right]\Phi(\vec{x}) = \Phi_S(\vec{x}) + \int_F \left[G(\vec{x},\vec{x}')\frac{d\Phi(\vec{x}')}{dn'} - \Phi(\vec{x}')\frac{dG(\vec{x},\vec{x}')}{dn'}\right] dS' \quad (1)$$

where Φ is the potential in the flaw region, G is the Green's function $[4\pi|\vec{x}-\vec{x}'|]^{-1}$, and F is the area around the flaw where the field is perturbed from the "no-flaw" solution. With Φ_{NF} denoting the field in the absence of a flaw, the source term in this equation is

$$\Phi_S(\vec{x}) = \Phi_0(\vec{x}) + \int_{S-F} \left[G(\vec{x},\vec{x}')\frac{d\Phi_{NF}(\vec{x}')}{dn'} - \Phi_{NF}(\vec{x}')\frac{dG(\vec{x},\vec{x}')}{dn'}\right] dS' \quad (2)$$

where Φ_0 is the probe field in free space and $S-F$ is the surface of the part outside the flaw region.

In this treatment, the field Φ_{NF} first was computed on the mesh shown in Figure 1. Then, with Φ_{NF} used to determine Φ_S, the potential in the flaw region was obtained by solving Eq. (1) on a much finer mesh that defined the flaw and the region influenced by the flaw. Calculation of the probe impedance involved two integrals, one over the flaw region and the other over the surface of the part outside the flaw region.

Calculation of the probe field Φ_0 also required a multistep approach. The first step was the determination of the free-space field produced by the two D-shaped windings on a BEM mesh defining the ferrite cores and shield. This calculation was done with a new model for coils of arbitrary shape, which is described elsewhere [5]. The fields on the surfaces of the ferrite pieces were computed next using a modified BEM code, and the free-space field for the whole probe then was given by an integral over the ferrite pieces plus the free-space field of the windings alone.

Figure 3 shows the free-space potential Φ_0 in a plane near the bottom of the probe. This plot is the result of a raster-like scan over the face of the probe, with curves generated by successive scans displaced upward for clarity. The figure shows the bipolar nature of the field of a differential probe, with positive peaks on one side of the double-D winding and negative peaks on the other side. In the actual calculations of probe impedance, Φ_0 was approximated by the field produced by a pair of oppositely directed dipoles, which closely resembled the data shown in Figure 3.

The modified BEM used for the probe calculation involved a new impedance boundary condition derived for nonconducting magnetic materials. The derivation [6] began with a calculation of the magnetic scalar potential on the surface of a linear magnetic half-space in the presence

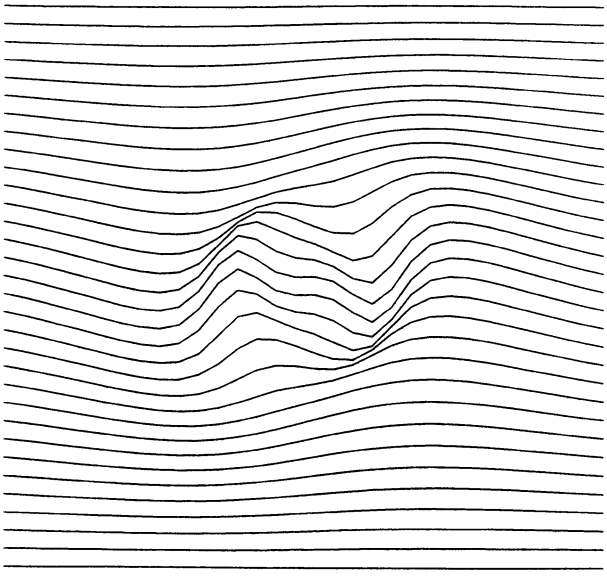

Fig. 3. Calculated magnetic scalar potential produced by the probe shown in Figure 2.

of an arbitrary current source above the half-space. In the limit as the conductivity of the material approaches zero, this solution was shown to yield the condition

$$\frac{d\Phi}{dn} = \frac{2\mu_r}{\mu_r + 1} \cdot \frac{d\Phi_0}{dn} \tag{3}$$

where Φ is now the potential on the half-space and Φ_0 is the free-space potential. The BEM code used for the probe calculations made use of this condition in place of the more familiar impedance boundary condition for conducting materials.

IMPEDANCE PREDICTIONS

Calculations were performed for a total of 30 scans, each consisting of 21 probe positions. Five equally spaced scan tracks were modeled, and the set of calculations included a part with no flaw, and parts with semicircular flaws of radius 0.76 mm and 1.27 mm. Two flaw positions were considered, one at the bottom edge of the beveled surface and the other in the center of that surface.

Figures 4 and 5 show typical results for the larger flaw size in the two flaw positions. The locus shown in Figure 4, obtained for a scan over the flaw in the center of the face, shows a rather distorted figure-8 pattern that is still recognizable as a flaw signal. In Figure 5, the scan is centered over the second flaw position in which the flaw intersects the edge at the end of the beveled surface. In this case, the severe distortion caused by the edge effect is evident. In fact, this result has very little difference from the impedance locus obtained with the same scan position in the absence of a flaw.

POD ANALYSIS

To obtain estimates of the probability of crack detection, impedance loci like those shown in Figures 4 and 5 were presented to two individuals experienced in eddy current inspection. These persons were shown the ideal figure-8 pattern expected in the presence of a flaw, and the distortion one should expect due to the edge effect. They were then asked to examine the impedance figures and determine which signals were indicative of flaws.

The results are summarized in Table 1. The POD estimate is the number of correct interpretations of flaw signals divided by the total number of scans over flawed regions. The probability of a false call is the number of incorrect flaw identifications divided by the number of scans over unflawed regions. Because of the limited number of scans examined,

Table 1. Detection Statistics

Flaw Radius (mm)	Probability of Detection
0.762	0.50
1.27	0.75

False Call Probability = 0.53

these results must be regarded as very cursory estimates of flaw detection statistics. Nevertheless, the results indicate a very poor detection probability and a very high false call rate, particularly for the smaller flaws. In fact, if the numbers shown in the table are taken at face value, they would say that the probabilities of flaw detection and false alarm are approximately equal for the smaller flaw, and that the chances of a correct interpretation are effectively random in this case. As was anticipated from an examination of the impedance data, the poor detection statistics obtained from this simulated inspection are due entirely to the proximity of the edge of the part to flaw locations.

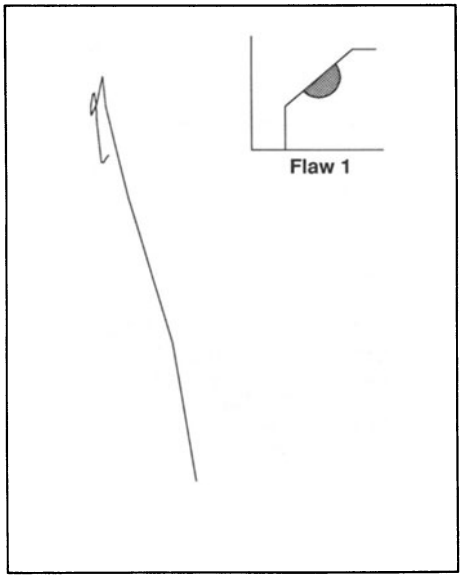

Fig. 4. Impedance locus for a scan over a flaw in the face of the beveled edge of the part shown in Figure 1. Horizontal and vertical axes are the real and imaginary parts, respectively, of the complex impedance.

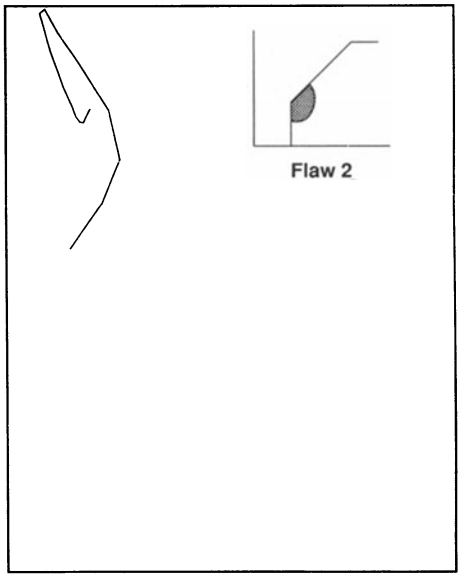

Fig. 5. Impedance locus for a corner flaw. The scale is the same as in Figure 4.

An independent experimental assessment of the POD also was carried out for the same part, probe, and inspection procedure, with much more favorable results [7]. The important difference between the experimental study and the computer simulation described here was that the part was machined prior to inspection to effectively remove the part edge from the region where flaws were expected to occur. The favorable results of the experimental study, along with the poor statistics obtained from the simulated inspection, suggest that the machining operation was effective in improving the probability of detection by minimizing the edge effect.

CONCLUSION

The calculations described in this paper serve as a demonstration of the feasibility of eddy current POD determination by computer simulation for complex part and probe geometries. This is not to say that the problem is now solved, and that eddy current modeling is ready for such applications on a routine basis. On the contrary, the calculations involved many approximations and the use of several different computer algorithms, some of which were developed specifically for this study. The work was a first attempt to piece together the various elements needed for a realistic, three-dimensional simulation of POD estimation; questions of accuracy of the various approximations were largely ignored in an effort to produce results in a reasonable period of time. The end result, therefore, is simply a feasibility demonstration. Considerably more effort will be required to develop tools that can be reliably used for eddy current POD estimation.

ACKNOWLEDGMENT

This work was sponsored by the Center for Advanced Nondestructive Evaluation, operated by the Ames Laboratory, USDOE, for the Air Force Wright Aeronautical Laboratories/Materials Laboratory under Contract No. W-7405-ENG-82 with Iowa State University.

REFERENCES

1. R. E. Beissner, "A Three-Dimensional Boundary Model for Eddy Current NDE," in Review of Progress in Quantitative NDE, edited by D. O. Thompson and D. E. Chimenti (Plenum, New York, 1989), Vol. 8, p. 229.
2. R. E. Beissner, K. A. Bartels, and J. L. Fisher, "Prediction of the Probability of Eddy Current Flaw Detection," in Review of Progress in Quantitative NDE, edited by D. O. Thompson and D. E. Chimenti (Plenum, New York, 1988), Vol. 7, p. 1753.
3. N. Nakagawa and R. E. Beissner, "Probability of Tight-Crack Detection Via Eddy Current Inspection," in these proceedings.
4. B. A. Auld, in Eddy-Current Characterization of Materials and Structures, ASTM STP 722, edited by G. Birnbaum and G. Free, American Society for Testing and Materials, Philadelphia (1981), p. 332.
5. R. E. Beissner and J. A. G. Temple, "Calculation of Eddy Current Fields for Coils of Arbitrary Shape," in these proceedings.
6. R. E. Beissner, to be published.
7. J. L. Fisher, G. L. Burkhardt, S. N. Rowland, Jr., J. H. Fitzgerald, R. J. Dexter, and J. P. Buckingham," Inspection Development for T-37 Wing Spar Cap Lug," Final Report SA-ALC/MMEP/88-02, prepared for San Antonio Air Logistics Center/MMEP, Kelly Air Force Base, Texas (1989).